INSOLATION-DRIVEN VARIABILITY IN DEBRIS-COVERED GLACIERS ON MARS AND EARTH. T. M. Meng, E. I. Petersen, and J. W. Holt, Lunar and Planetary Laboratory, University of Arizona (tmeng@email.arizona.edu)

Introduction: Debris-covered glaciers (DCG) play a unique but important role in the long-term preservation of ice on Mars and Earth. This ice preservation stores information about paleoclimate [1] and it sequesters significant stores of water that contribute to hydrological resources in alpine communities on Earth and are strong candidates for *in situ* resource utilization on Mars due to their large volume, high ice concentration, and relatively low latitude [2,3]. The supraglacial debris layer is a key component of DCG on both Earth and Mars. It provides a thermal boundary that shields water ice in regions where it would be unstable at the ground surface.

While the supraglacial debris plays a significant role in the preservation of the ice in DCG, the lack of radar sounding detections of the debris/ice interface on Mars leaves many key properties—including the thickness—of this debris layer poorly constrained [4]. Vapor diffusion models constrained by gamma ray spectrometer data indicate depths to ice stability greater than one meter at the mid-latitudes [5], but the theoretical vertical resolution of the Shallow Radar (SHARAD) instrument is approximately 10 m in geologic media [6].

Additionally, multiple glacier flow models inverting surface slope with SHARAD-derived basal topography indicate heterogeneities in viscous yield stresses and creep parameters between the pole- and equator-facing slopes of a DCG in Mars' southern hemisphere [7, 8, 9]. This trend may be analogous on Earth; change-detection measurements show that a pole-facing DCG in Alaska flows approximately half the speed of its equator-facing neighbor. In consideration of the gap in near-surface data for Mars along with the observation of heterogeneous DCG flow on Earth, here we test the hypothesis that topography causes significant variation in solar radiation received between equator- and pole-facing slopes, which may be sufficient to drive variations in viscous flow or depth to stable ice.

Method – Annual Insolation Ratios: To test the variation in solar insolation with slope aspect, we calculated the apparent horizon from the perspective of individual DCG using Shuttle Radar Topography Mission (SRTM) data for Earth (~10 m/pixel) and Mars Orbiter Laser Altimeter (MOLA) data for Mars (~400 m/pixel). We calculated one horizon for each DCG lobe shown in Figure 1a and each view point in Figure 1b. Next, we compared this horizon with the predicted path of the sun and estimated the amount of radiation obstructed by the true horizon in comparison with a flat horizon.

Since annual solar path depends on the planet's spin axis obliquity, and Mars' obliquity varies with high amplitude [10], we estimated the variation in insolation at present day obliquity (25°) and high obliquity (40°). Our estimations produce relative insolation ratios (Q_{rg}/Q_{flat}) at localized coordinates, therefore we do not consider deviations in orbital distance or absolute heat flux.

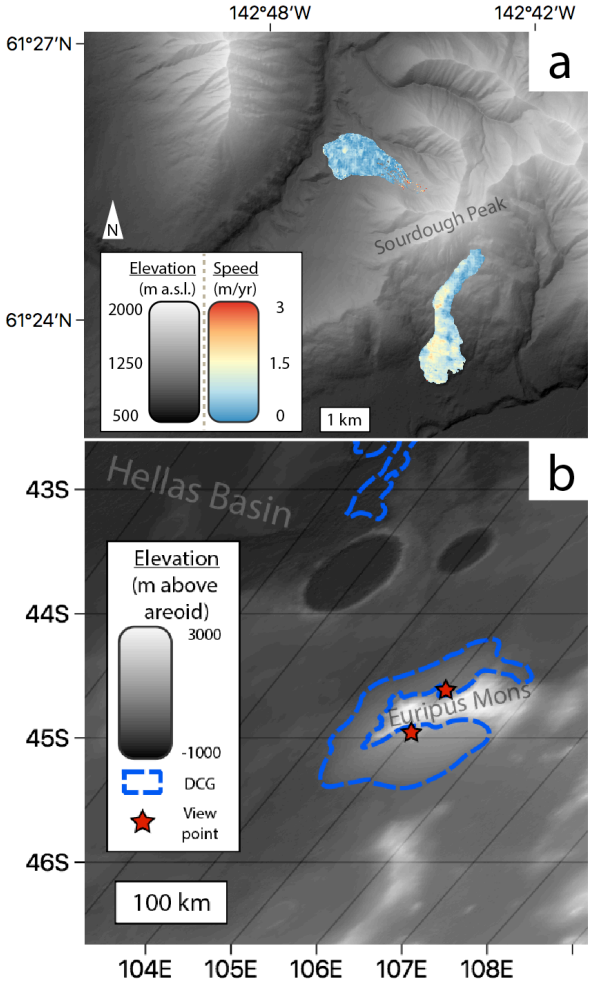

Figure 1: a) Map showing hillshaded SRTM 1/3'' elevation data published with the U.S. National Elevation Dataset along with repeat photogrammetry change detection measurements of two DCG in the Wrangell Mountains, Alaska. The equator-facing DCG flows approximately twice as fast as the pole-facing DCG [11]. b) Locations of view points used to plot apparent horizons on Euripus Mons, Mars with the context of MOLA elevation data and the DCG mapped in [2] and modeled in [7, 8, 9].

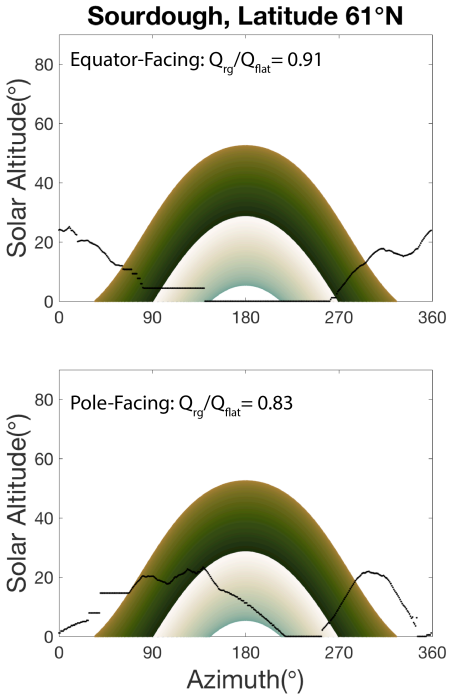

Figure 2: Visualization of annual sun path versus apparent horizon comparison for two DCG in Alaska: horizon is shown in black, sun path is plotted in green above the equinox, and off-white below the equinox. Relative annual solar radiation is calculated by removing insolation contribution if sun angle is less than horizon angle; time step is one minute. North azimuth is 0° and 360°.

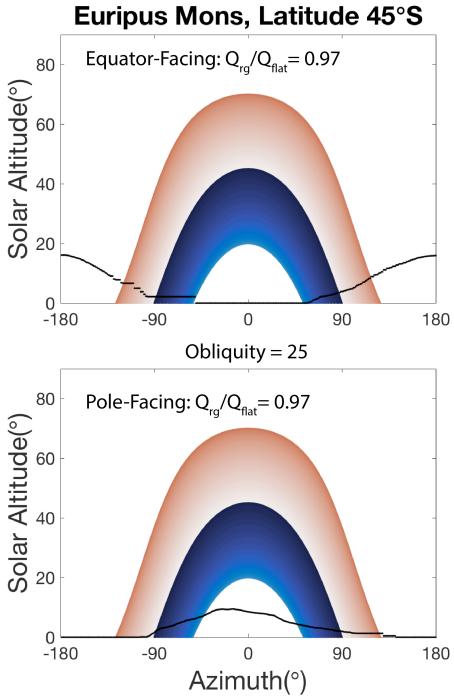

Figure 3: Sun path/horizon plot for Euripus Mons, Mars at the current obliquity, where the horizon is plotted in black, above the equinox is red, and below the equinox is blue. South azimuth is -180° and 180°.

Result – Extreme Topography Required: Figure 2 shows that for the terrestrial case, the equator-facing DCG receives 91% of the radiation of a flat horizon at that geographic location, while the pole-facing DCG receives 83%. These results suggest a measureable difference in solar radiation between the neighboring DCG, and future work should consider this difference in heat flux when modeling glacier strain rate or viscosity at these sites. Conversely, the martian site of interest does not have discernible radiation differences between the equator- and pole-facing slopes at the current obliquity (Figure 3), and has a 1% difference at high obliquity. While Euripus Mons is a significant massif, the low average DCG surface slopes of ~2° and wide lateral extent ensure that the line of sight that produces the apparent horizon remains at a low altitude angle, therefore obstructing less intense sunlight in comparison with the terrestrial analogs, where surface slopes typically exceed 10°.

Discussion – Accumulation vs. Insolation: While the results for the terrestrial sites show that extreme topographic relief between two DCG can cause insolation differences that may explain observed differences in present-day flow, the martian sites did not display this same variability. This implies that observed differences in glacier properties are not a product of the insolation regime of the present day. Rather, it suggests that the differences must have been caused by local variations in ice accumulation at the time of glaciation, which is driven by global and regional climates instead of directly through astronomical parameters. This conclusion indicates that *slope aspect is not a robust indicator of current depth to ice stability* for the largest DCG on Mars. More data and analyses are needed to confidently characterize fine-scale variations in the supraglacial debris layer, glacier flow parameters, and emplacement history.

References: [1] Mackay S. L. and Marchant D. R. (2017) *Nature Comms., 8,* 14194. [2] Levy J. S. et al. (2014) *JGR Planets, 119,* 2188-2196. [3] Petersen E. I. et al. (2018) *GRL, 45,* 11595–11604. [4] Baker D. M. H. and Carter L. M. (2019) *Icarus, 319,* 745-769. [5] Aharonson O. and Schorghofer N. (2006) *JGR Planets, 111,* E110077. [6] Seu R. et al. (2007) *JGR Planets, 112,* E05S05. [7] Karlsson N. B. et al. (2015) *GRL, 8*, 2627-2633. [8] Parsons R. and Holt J. W. (2016) *JGR Planets, 121*, 432-453. [9] Schmidt L. S. et al. (2019) *J. Glaciology*, 1-11. [10] Laskar J. et al. (2004) *Icarus, 170*, 343-364. [11] Meng T. M. et al. (2019) *LPSC 50*, Abstract #3197.